Anal. Chem. **2004,** *76,* 2575−2582

Calibration-Free Estimates of Batch Process Yields and Detection of Process Upsets Using in Situ Spectroscopic Measurements and Nonisothermal Kinetic Models: 4-(Dimethylamino)pyridine-Catalyzed Esterification of Butanol

Paul Gemperline,*,† Graeme Puxty,‡ Marcel Maeder,‡ Dwight Walker,§ Frank Tarczynski,§ and Mary Bosserman†

Department of Chemistry, East Carolina University, Greenville, North Carolina 27858, Department of Chemistry, University of Newcastle, Newcastle, NSW, Australia, and GlaxoSmithKline, 5 Moore Drive, Research Triangle Park, North Carolina 27709

In this paper, we report the use of an NIR fiber-optic spectrometer with a high-speed diode array for calibration-free monitoring and modeling of the reaction of acetic anhydride with butanol using the catalyst 4-(dimethylamino)pyridine in a microscale batch reactor. Acquisition of spectra at 5 ms/scan gave information relevant for modeling these fast batch processes with a single multibatch kinetic model. Nonlinear fitting of a first-principles model directly to the reaction spectra gave calibration-free estimates of time-dependent concentration profiles and pure component spectra. The amount of catalyst was varied between different batches to permit accurate estimation of its effect in the multiway model. A wide range of different models with increasing complexity could be fit to each batch individually with low residuals and apparent low lack of fit. However, only one model properly estimated the concentration profiles when all five batches were fitted simultaneously in a multiway kinetic model. Inclusion of on-line temperature measurements and use of an Arrhenius model for the estimated rate constant gave significantly improved model fits compared to an isothermal kinetic model. Augmentation of prerun batches with data from an additional batch permitted model-based forecasts of reaction trajectories, reaction yield, reaction end points, and process upsets. One batch with added water to simulate a process upset was easily detected by the calibration free process model.

During the last 20 years, a dramatic increase has been observed in the use of process analytical chemistry (PAC) to monitor and control modern chemical processes. PAC techniques employ on-line sensors to measure physical properties of processes in real time. There has been an increasing trend toward the use of multivariate sensors, such as fiber-optic spectrometers, capable of rapidly measuring the optical properties of process streams and batches over a large spectral range with high signal-to-noise ratios. The large volume of data produced by these instruments has typically been used to develop multivariate calibration models using techniques such as principal component regression[1] and partial least squares (PLS).[2−4] The major goals of these types of applications are to detect and diagnose process upsets and monitor product quality and yield.[5] In some cases, the output of the calibration model is used for feedback control.[5] One drawback of the multivariate calibration approach is that a significant amount of effort is required to develop and maintain the calibration model. For example, instrument maintenance events (lamp changes, fiber replacement, etc.) or process changes (change in raw material suppliers or product formulation) may degrade or even invalidate a calibration model, requiring a significant amount of effort to update or revise it.

For batch chemical processes, fitting of a first-principles kinetic model offers a calibration-free approach to monitoring and modeling that does not require the significant effort of multivariate calibration. In this approach, a reaction mechanism is postulated giving a system of simultaneous ordinary differential equations (ODEs). Using known initial conditions, the ODEs are numerically integrated to estimate time-dependent concentration profiles. The concentration profiles are fitted directly to the reaction spectra by nonlinear optimization of the rate constants. Neither calibration spectra nor off-line reference measurements are required in the model-fitting process. For process analysis applications, approximate model parameters, in the form of rate constants can be determined from prerun batches. During subsequent batch runs, the prerun batch spectra can be augmented with the new batch spectra as they are acquired. The model parameters can then be updated in real time by nonlinear fitting methods and used to monitor the progress of the batch, detect process upsets, and forecast batch end points, product yield, and product quality.

* To whom correspondence should be addressed. E-mail: gemperlinep@mail.ecu.edu.

† East Carolina University.

‡ University of Newcastle.

§ GlaxoSmithKline.

(1) Wise, B. M.; Gallagher, N. B. *J. Process Control* **1996**, *6*, 329−348.

(2) Kourti, T.; MacGregor, J. F. *Chemom. Intell. Lab. Syst.* **1995**, *28*, 3−21.

(3) Nomikos, P.; MacGregor, J. F. *Chemom. Intell. Lab. Syst.* **1995**, *30*, 97−108.

(4) Burnham, A. J.; Viveros, R.; MacGregor, J. F. *J. Chemom.* **1996**, *10*, 31−45.

(5) Wise, B. M.; Ricker, N. L. *AIChE Symp. Ser.* **1989**, *85*, 19−23.

10.1021/ac035356i CCC: $27.50
Published on Web 03/27/2004

Changes in instrument response due to maintenance events such as lamp changes are inconsequential as long as the instrument response continues to provide sufficient signal to accurately and precisely update parameter estimates.

Traditional near-infrared (NIR) measurements have found widespread use in process analytical application because of the method's good sensitivity, high information content, and low noise. Commercially available scanning instruments or Fourier transform (FT-NIR) instruments require long scan times. Some batch processes take place on a much shorter time frame. For example, 4-(dimethylamino)pyridine (DMAP) is one of the best-known catalysts available for acetylation with acetic anhydride, and commercially available NIR scanning or FT instruments may be too slow to give measurements relevant for estimation of rate constants. Recent advances in semiconductor technology has made possible indium gallium arsenide charge-coupled device diode arrays with excellent sensitivity in the range from 1100 to 2200 nm and high scan speeds of 5 ms.[6]

In this paper, we report the use of an NIR fiber-optic spectrometer with a high-speed diode array for monitoring and modeling the reaction of acetic anhydride and butanol with DMAP as the catalyst in a microscale batch reactor. The spectrometer is capable of acquiring spectra at the rate of 5 ms/scan, which gives information relevant for modeling the batch process with a kinetic model. A total of five different batches were modeled in a multiway kinetic model. Augmentation of four prerun batches with data from a fifth batch permitted updating of parameter estimates as well as forecasting reaction trajectories, reaction yield and end points.

Data Analysis Method. The use of multivariate absorption measurements for fitting multiway kinetic models has received considerable attention in the past few years.[7−10] In most of these approaches, nonlinear least-squares estimation of model parameters is required. In this paper we chose the nonlinear least-squares (NLLS) Levenberg−Marquardt algorithm[11] to fit the activation parameters of our proposed reaction mechanism using a hard-modeling approach. The NLLS fitting of multivariate absorption data has been used for some time,[12] and the procedure is briefly outlined here.

The on-line spectroscopic measurements consist of s spectra measured at w wavelengths arranged into a data matrix $\mathbf{Y}$ with dimensions $s \times w$. According to the Beer−Lambert law, this matrix can be decomposed into the product of a concentration matrix $\mathbf{C}$ ($s \times n$) and a matrix of molar absorptivities $\mathbf{A}$ ($n \times w$), where n is the number of absorbing species.

$$\mathbf{Y} = \mathbf{CA} + \mathbf{R} \tag{1}$$

However, due to the noise inherent in any measurement and other sources of measurement error such as concentration errors, this decomposition does not represent $\mathbf{Y}$ exactly. We define a residuals matrix $\mathbf{R}$ that is the difference between the measurements and the model. The process of nonlinear least-squares fitting gives estimates $\hat{\mathbf{C}}$ and $\hat{\mathbf{A}}$ that best represent $\mathbf{Y}$ by minimizing the sum of squares of the residuals matrix $\hat{\mathbf{R}}$.

$$\hat{\mathbf{R}} = \mathrm{Y} - \hat{\mathbf{C}}\hat{\mathbf{A}} \tag{2}$$

Calibration-free modeling of batch reactions is summarized by the following steps: (1) A reaction mechanism is postulated giving a model composed of a system of simultaneous ODEs. (2) Numerical integration of the ODEs produces an estimate of $\hat{\mathbf{C}}$. (3) Least-squares fitting of $\hat{\mathbf{C}}$ to $\mathbf{Y}$ produces calibration-free estimates of pure component spectra, $\hat{\mathbf{A}}$. (4) The model parameters (rate constants) are iteratively adjusted by a nonlinear estimation method until no further reduction in $\hat{\mathbf{R}}^2$ is obtained.

Specialized software with a graphical user interface was written in C++ to perform the kinetic modeling. After postulating a chemical model, it is encoded into strings of text representing the proposed reaction mechanism and input into the computer program. For example, the reaction between acetic anhydride and butanol might be represented by the following string: "AcOAc + BuOH + DMAP > BuOAc + HOAc + DMAP". The program uses an intelligent model parser to extract the number of species, species names, their corresponding stoichiometric coefficients, and the number of reactions. The program produces a list of parameters, their reaction coefficients and constructs a system of ODEs that describes the change in concentration of each species with time.[13] This approach is completely general so that a system of ODEs of arbitrary complexity can be automatically generated for any number of coupled reactions. With knowledge of the initial concentrations of the species in the chemical model, the differential equations are integrated to yield the concentration of each species at any desired time. Only the simplest system of ODEs describing chemical models can be integrated explicitly; consequently, the Bulirsch−Stoer numerical integration technique was used,[11] which is capable of integrating complex systems of stiff ODEs to any desired level of accuracy.

The parameters to be fitted associated with a chemical model are the rate constants of each step. Under isothermal conditions, it is assumed that the rate constants of all reaction steps remain constant for all experiments. The experiments reported in this paper were performed under nonisothermal conditions, necessitating the use of the Arrhenius model to describe the rate constants, k, as a function of the absolute temperature, T:

$$k = A\mathrm{e}^{-E_\mathrm{A}/RT} \tag{3}$$

where A is the preexponential factor, E_A is the activation energy of the reaction, and R is the universal gas constant. The two fitted parameters, A and E_A, are different by several orders of magnitude in most typical applications, which causes significant problems during nonlinear estimation. To alleviate this problem, the Arrhenius equation was reparametrized to the form shown in eq 4,

(6) Hoogeveen, R. W. M.; van der A, R. J.; Goede, A. P. H. *Infrared Phys. Technol.* **2001**, *42*, 1−16.
(7) Dyson, R.; Maeder, M.; Neuhold, Y.-M.; Puxty, G. *Anal. Chim. Acta* **2003**, *490*, 99−108.
(8) Neuhold, Y.-M.; Maeder, M. *J. Chemom.* **2002**, *16*, 218−227.
(9) Bijlsma, S.; Louwerse, D. J.; Smilde, A. K. *J. Chemom.* **1999**, *13*, 311−329.
(10) Bijlsma, S.; Louwerse, D. J.; Windig, W.; Smilde, A. K. *Anal. Chim Acta* **1998**, *376*, 339−355.
(11) Press, W. H.; Flannery, B. P.; Teukolsky, S. A.; Vetterling, W. T. *Numerical Recipes in C: The Art of Scientific Computing*; Cambrige University Press: Cambridge, U.K., 1992.
(12) Maeder, M.; Zuberbühler, A. D. *Anal. Chem.* **1990**, *62*, 2220−2224.
(13) Dyson, R.; Maeder, M.; Puxty, G.; Neuhold, Y.-M. *Inorg, React. Mech.* In press.

$$k = k_{\mathrm{ref}} e^{-(1/T - 1/T_{\mathrm{ref}})E_A/R} \quad (4)$$

where k_{ref} is the rate constant at temperature T_{ref}. This form of the Arrhenius model was used during nonlinear least-squares fitting to reduce correlation between the parameters A and E_A, thereby improving nonlinear fitting performance.[14] Once fitting was complete, a straightforward calculation was used to recover A from k_{ref} and T_{ref}.

Before nonlinear model fitting was performed, starting conditions were specified, e.g., the initial concentrations of the species involved in the reactions and initial estimates for the model parameters k_{ref} and E_A. Numerical integration of the system of simultaneous ODEs to the spectral acquisition times was performed with these initial estimates and the known initial concentrations to calculate the time-dependent matrix of concentration profiles, $\hat{\mathbf{C}}$. After integration, calibration-free estimates of the molar absorptivities, $\hat{\mathbf{A}}$, were obtained by a linear regression step,[12] where $\hat{\mathbf{C}}^+$ is the pseudoinverse $\hat{\mathbf{C}}$.

$$\hat{\mathbf{A}} = \hat{\mathbf{C}}^+ \mathbf{Y} \quad (5)$$

The Levenberg−Marquardt method of nonlinear least squares was used to minimize the sum of squares of the resulting residuals, $\hat{\mathbf{R}}$, by iteratively adjusting the nonlinear parameters k_{ref} and E_A.

$$\hat{\mathbf{R}} = \mathbf{Y} - \hat{\mathbf{C}}\hat{\mathbf{A}} \quad (6)$$

To achieve a more robust fit with reduced correlation between the nonlinear parameters and also to take advantage of the fact that a number of separate experiments were made under different initial conditions, fitting was carried out in a second-order global analysis mode.[15,16] In this mode, a global chemical model was fitted simultaneously to all the experiments. Ideally, a single matrix of molar absorptivities would be calculated in such an analysis; however, due to baseline shifts between measurements, it was necessary to calculate individual $\hat{\mathbf{A}}$ for each experiment. Furusjö et al.[14] have carried out similar fitting of nonisothermal in situ infrared and Raman measurements. They argued for a different function to be minimized:

$$\hat{\mathbf{R}} = (\mathbf{I} - \mathbf{U}\mathbf{U}^{\mathbf{T}})\hat{\mathbf{C}} \quad (7)$$

where $\mathbf{U}$ contains the trimmed set of left eigenvectors from the singular value decomposition of $\mathbf{Y}$. For nonisothermal data, the advantage of this function is that it is resistant to absorption peak shifts with temperature that may occur for mid-IR and Raman data. This function, however, relies on the assumption that $\hat{\mathbf{C}}$ is contained in the space spanned by the columns of $\mathbf{U}$. This is only true near the optimum solution, suggesting that if poor initial parameter estimates are used, the routine may struggle to converge to the correct $\mathbf{C}$. To test this hypothesis, we implemented this alternative merit function and found it to be very sensitive to the initial parameter estimates. Even for a simple simulated second-order reaction, where a single parameter was fitted, it converged to the correct value only when the initial parameter estimate was close to the optimal value, whereas using function 6 resulted in convergence from a broader range of initial estimates. Also, we found function 7 to be very sensitive to the number of significant eigenvectors used. When applied to the nonisothermal data, the fitted activation parameters did not agree with those from the NLLS fit and produced unrealistic values. Furthermore, the quality of the NLLS fits using function 6 indicated that the measured data were not suffering from any significant systematic deviations from the model estimated measurements.

(14) Furusjö, E.; Svensson, O.; Danielsson, L.-G. *Chemom. Intell. Lab. Syst.* **2003**, *66*, 1−14.
(15) Bugnon, P.; Chottard, J.; Jestin, J.; Jung, B.; Laurenczy, G.; Maeder, M.; Merbach, A. E.; Zuberbühler, A. D. *Anal. Chim Acta* **1994**, *298*, 193−201.
(16) Dyson, R. M.; Kaderli, S.; Lawrance, G. A.; Maeder, M.; Zuberbühler, A. D. *Anal. Chim.* **1997**, *353*, 381−393.

EXPERIMENTAL SECTION

Equipment. All reactions were performed in an auto-MATE reactor system (H.E.L. Inc., Lawrenceville, NJ), a miniature (50 mL) computer-controlled multiple reactor system. Process conditions, including reaction temperature, jacket temperature, and agitation, were controlled by WinISO software from H.E.L. running on a 333-MHz Pentium II computer. The heads of the auto-MATE reactors were modified to accept fiber-optic retroreflection Near-IR probes from Equitech International (New Ellenton, SC).

Near-IR spectra were collected over the range of 1400−2100 nm using a CP-140 short focal length, 140 mm, near-IR fiber-optic spectrophotometer fitted with a 120 grove/mm grating (JY Horiba, Edison NJ) coupled to a high-speed 256-element, InGaAS array from Hamamatsu (Bridgewater NJ). Near-IR illumination was provided by a tungsten filament lamp and adjustable power supply (Thermo Oriel, Stratford CT). The retroreflection probe had a 1-mm path length housed in a stainless steel probe 12.5 mm in diameter and 140 mm in length. The probe was fitted with two 400-μm core low-OH fused-silica fibers.

Spectrometer data acquisition was performed using in-house-written software using LabVIEW version 6 software (National Instruments, Austin TX) and an instrument control library supplied by Hamamatsu. The power supplied to the lamp was adjusted to ensure optimum use of the diode array and A/D converter dynamic range with a maximum digitized intensity in the range of 6.5×10^4 counts.

Reaction Conditions. The reaction used to study the capabilities of the combined calorimeter/NIR spectrograph and batch analysis software was the acetylation of 1-butanol with acetic anhydride with DMAP as a catalyst. A 20-mL aliquot of anhydrous 1-butanol (Aldrich Milwaukee, WI) and 21 mL of acetic anhydride (Aldrich) were added to a dry 50-mL reactor at room temperature. (Warning, acetic anhydride is a corrosive and combustible liquid, incompatible with strong oxidizing agents, water, strong bases, and alcohols). All reagents came from freshly opened bottles. The reactor jacket was cooled to −25 °C, and power was applied to the internal reactor heater to warm the contents to 20 °C. Accurately weighted amounts of DMAP in the range of 20−80 mg (Aldrich) were added directly into the glass reactor vessel to initiate the reaction. Near-IR spectra were collected every second using a dry N_2 reference. The reactions were run until the solution temperatures returned to 20 °C. An additional two reactions were performed with 400 and 800 μL of water added to the reactor prior to initiation of the batch reaction to simulate process upsets. An

Table 1. Reaction Conditions and Model Estimated Initial Rates[a]

batch	mass DMAP (mg)	concn DMAP (mol L^{-1})	initial rate at 20 °C (mol L^{-1} min^{-1})	exotherm range (°C)
1	80.6	0.0160	1.22	19.7−32.9
2	51.7	0.0102	0.783	19.5−26.5
3	53.1	0.0105	0.804	19.3−26.4
4	55.0	0.0109	0.833	19.7−27.6
5	21.2	0.00420	0.321	20.0−21.7

[a] Initial concentration of acetic anhydride and butanol for all batches was 5.41 and 5.33 mol/L, respectively. The mass of DMAP added was varied.

unexpected absorption band was observed in the batch with 400 μL of water that suggested some additional source of contamination besides water was present; thus, it was not used in the calculations described below.

RESULTS

A third-order reaction mechanism (8) was fitted to all five batches simultaneously. The initial conditions for each batch are listed in Table 1. There is some error in the determined initial concentrations as no consideration was given to the change in density of the reactants after mixing. The catalyst, DMAP, was included in the mechanism as it had a different initial concentration for each batch. Its inclusion was necessary to fit the model simultaneously to all batches. Even though the reaction is third order overall, in each batch, the reaction is effectively pseudo second order because DMAP is liberated at the same rate at which it is consumed, thereby causing the concentration of DMAP to remain fairly constant throughout the course of the reaction.

$$\mathrm{AcOAc} + \mathrm{BuOH} + \mathrm{DMAP} \rightarrow \mathrm{BuOAc} + \mathrm{AcOH} + \mathrm{DMAP} \quad (8)$$

The amount of DMAP was varied over a wide range between batches, giving significantly different initial rates and significantly different reaction exotherms. For example, the initial reaction rate estimated for batch 1 was 1.22 and 0.321 mol L^{-1} min^{-1} for batch 5. The starting temperature for each batch was ∼20 °C. The peak temperature during batch 1 reached 32.9 °C, whereas the peak temperature was only 21.7 °C for batch 5. This is remarkable considering the reactor jacket was chilled to −25 °C and the reactor set point was 20 °C. At steady-state conditions, the reaction calorimeter heater controller supplied ∼18 W of power to the auxiliary heater in the reactor to maintain this temperature differential. During batch 1, the evolution of heat from the chemical reaction was sufficiently rapid that the controller reduced the auxiliary heater power to zero for nearly 3 min and still the heat removed by the jacket at −25 °C was insufficient to maintain constant temperature.

Fitting the postulated model shown in eq 8 to each experiment individually did not provide sufficient information to simultaneously estimate k_{ref} and E_A with good reliability, except for batch 1. The relatively large exotherm of batch 1 ensured good observability for E_A and was defined by this batch alone, whereas,

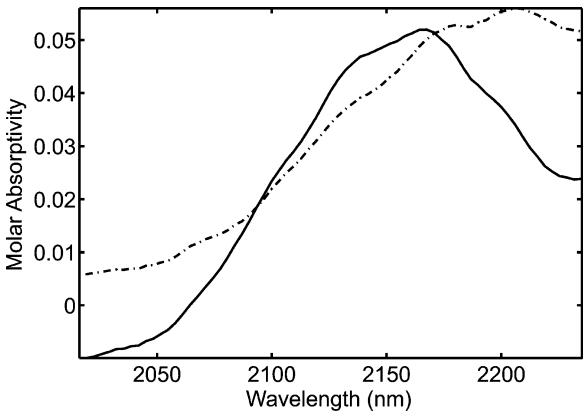

Figure 1. Estimated pure component spectra for 80.6-mg batch. The solid line is a combined spectrum for the reactants (acetic anhydride and butanol), and the dash−dot line is the products (acetic acid and butyl acetate).

batches 2−5 had smaller exotherms. Furthermore, a wide range of different models with increasing complexity could be fit to each batch individually with low residuals and apparent low lack of fit. However, only the model described in eq 8 estimated the concentration profiles with low residuals for all five batches simultaneously in a multiway kinetic model. As expected, fitting one model simultaneously to many different experiments permitted elimination of incorrect models and unambiguous identification of the correct model; this is due to the increased robustness on globalized analyses.

Ideally if there are no baseline shifts or other spectroscopic changes between batches, it is possible to estimate a single matrix of pure component spectra in the linear least-squares step described in eq 5. However, it was apparent there were both baseline shifts and other spectral inconsistencies between batches, which was not unexpected since a single-fiber NIR probe was used. Single-fiber probes tend to be sensitive to changes in fiber position that can sometimes produce different amounts of baseline offset. While we were able to remove the baseline shift between batches,[17] small spectral inconsistencies between batches were still apparent. In this circumstance, it was necessary to use a local spectral model for each batch instead of a global spectral model. In a local spectral model, the estimated pure spectra are allowed to be different from batch to batch. Also a reduced wavelength range was used for fitting, 2016.2−2235.1 nm, to avoid regions where obvious instrumental inconsistencies occurred such as no signal or large noise spikes. The estimated pure component spectra for the 80.6-mg batch are shown in Figure 1. The negative regions are due to the presence of small, negative absorption measurements in the measured reaction spectra. The estimated pure component spectra for the other batches are very similar but show some minor differences. Additionally, the first 30 s of measurements from each batch was excluded from fitting. This was to allow for the dissolution and mixing of DMAP since it was added as a solid.

The fitted preexponential factor and activation energy and their respective uncertainties are listed in Table 2. We found the minimum to be well defined with the NLLS routine converging

(17) Maeder, M.; Neuhold, Y.-M.; Olsen, A.; Puxty, G.; Dyson, R.; Zilian, A. *Anal. Chim.* **2002**, *464*, 249−259.

Table 2. Fitted Values for the Preexponential Factor and the Activation Energy[a]

A ($L^2mol^{-2}min^{-1}$)	E_A (kJ)
$1.94 \times \mathbf{10^7}$ (1)	38.5 (2)

[a] Uncertainties are given in parentheses and represent two standard deviations of the last significant digit.

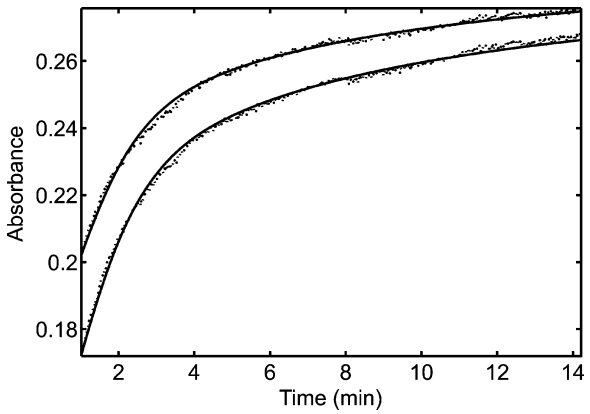

Figure 2. Nonisothermal fits at 2202.9 (upper) and 2212.6 nm (lower) for 80.6 mg of DMAP. The dotted lines are the measured data and the solid lines the calculated data.

to the listed values from a number of different initial starting points. This fact, coupled with the excellent quality of the fits (0.5% RSD in the fitted parameters, k_{ref} and E_A, 0.5% RSD in fitted absorbance values), indicates the observability of the estimated parameters was excellent. The listed uncertainties are estimated by statistical means, assuming a local linearization of the nonlinear model near the minimum gives a good approximation to the actual error covariance matrix.[11] They are most certainly an underestimate of the true uncertainties as no account has been taken of departures from the above assumptions or the presence of experimental errors such as those in mass and volume. The quality of the fit is good, and representative fits at two different wavelengths are shown in Figure 2. The overall standard deviation in the residuals from the fit was 1.13×10^{-3} absorbance units, which is well within the instrumental noise level. A plot of the estimated reaction profiles is shown in Figure 3.

To illustrate the benefit of fitting the activation parameters with an Arrhenius model, we also carried out the fit by assuming isothermal conditions. In this situation, only a rate constant is fitted rather then the activation parameters of the Arrhenius equation. The fitted rate constant is assumed to be invariant throughout the reaction. Figure 4 shows the temperature profile for the 80.6-mg batch and fits at the same wavelengths as Figure 2, assuming isothermal conditions. The isothermal model underestimates the initial reaction rate early in the batch when the temperature is higher and overestimates the rate later in the batch when the temperature is lower. This illustrates the benefit of incorporating temperature into the model.

Prediction of Batch 5 from Batches 1−4. To illustrate the use of kinetic modeling to forecast batch profiles and detect batch end points, a kinetic analysis of batches 1−4 was performed (see Table 3). The resulting model was used to forecast the reaction profiles for batch 5. A significantly lower level of catalyst not represented in the training batches was used for batch 5; thus, the forecast of batch 5 reaction profiles represents an extrapolation of the model to new conditions. Slightly different parameter estimates for the preexponential factor, A, and the activation energy, E_A, were obtained when only batches 1−4 were included in the model-fitting procedure. However, accurate predictions of batch 5 concentration profiles were obtained (see Table 4). At 15.67 min, the model forecasted concentration of reactants and product deviated from the values obtained from the full model by less than 2%.

Detection of Process Upsets. To illustrate the use of kinetic modeling for detecting process upsets, a kinetic model was fitted to batches 1−5 plus one batch with 55.1 mg of DMAP catalyst and 800 μL of adder water to simulate a process upset. The addition of the 800 μL of water resulted in a significant change to the model-estimated parameters, the overall standard deviation, and the estimated pure component spectra (see Table 5).

Additionally, the standard deviation of the residuals for the adulterated batch was significantly larger than for the other batches, indicating the adulterated batch deviates from the batches 1−5. Examination of the estimated pure component spectra revealed that the spectra of the adulterated batch differ significantly from those of the five good batches. The most obvious difference is that the adulterated batch contains an additional peak due to water. Part of the peak can be seen at the lower wavelengths in Figure 5.

Speed of Process Upset Detection. To study the speed at which process upsets can be detected by kinetic modeling, the model parameters were fixed at the values determined for the five good batches. Spectra were then added from the adulterated batch one at a time until enough spectra were present such that detection of a process upset was evident. The first 30 s of data from the adulterated batch was omitted to allow for DMAP mixing times and to remain consistent with the data analysis of the five good batches. Following the addition of two spectra, the standard deviation of the residuals for the spectra from the adulterated batch was 6.25×10^{-3}, ~6 times that of the overall standard deviation prior to the addition of the spectra from the adulterated batch. The standard deviation of the spectra from the adulterated batch remained high, about 4−5.5 times greater than the overall standard deviation prior to the addition of the adulterated batch. The presence of the process upset is detected after the inclusion of two spectra from the adulterated batch.

CONCLUSIONS

In this paper, we have demonstrated that fitting multivariate kinetic models to in situ spectroscopic measurements can be a powerful calibration-free tool for batch process monitoring and control. First-principles models coupled with in situ spectroscopic measurements can be used to determine reaction mechanisms, time-dependent batch concentration profiles, reaction yields, and reaction end points. Costly, time-consuming off-line reference measurements with multivariate calibration methods such as PLS) are not required to obtain accurate real-time estimates of concentration profiles. Real-time modeling of a batch reaction can be achieved by augmenting prerun batch data with recently acquired spectral data followed by fitting of a multiway kinetic model. In real-time applications, accurate initial guesses of the parameter

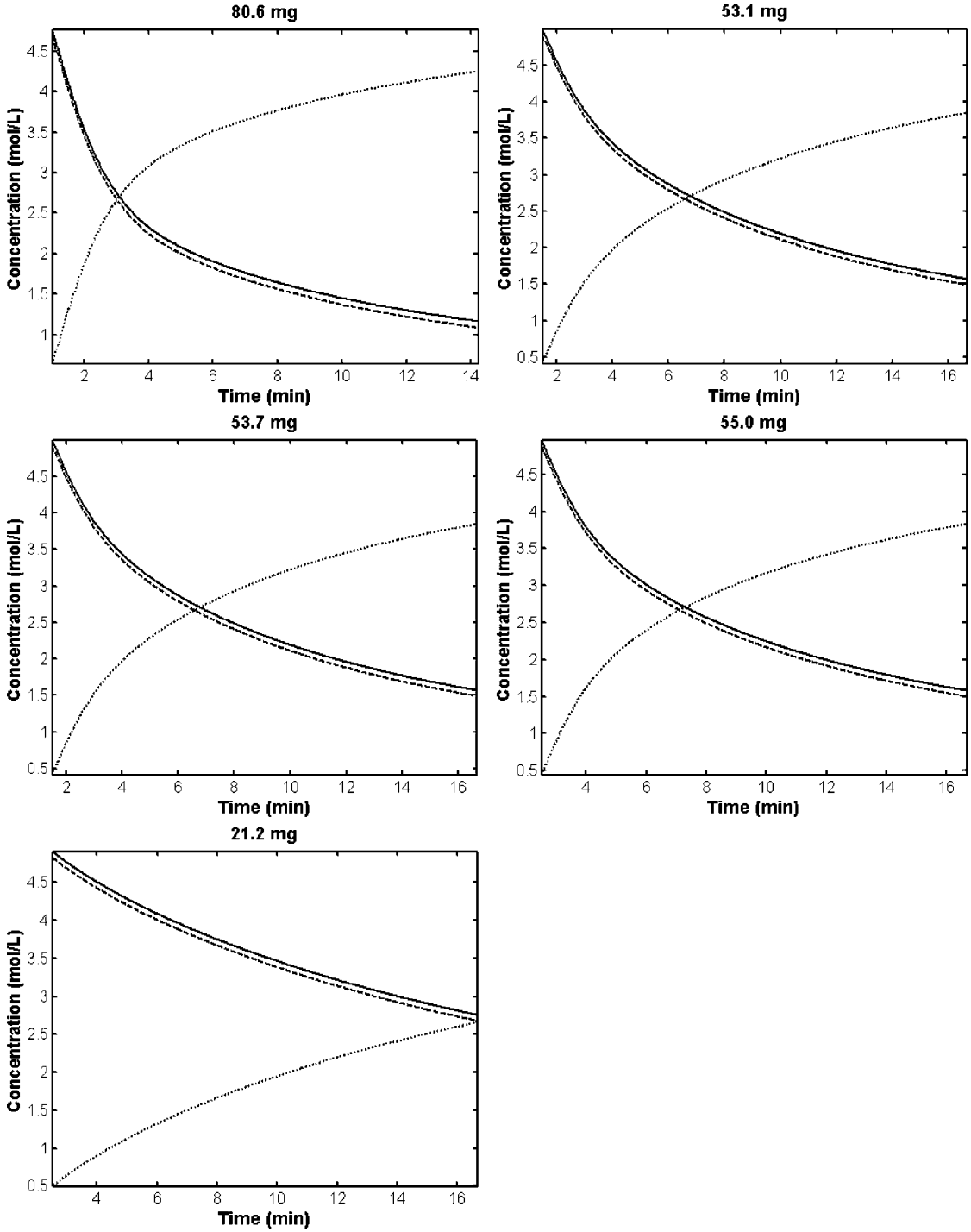

Figure 3. Estimated reaction profiles of acetic anhydride (—), butanol (– –), and acetic acid and butyl acetate (••) for five batches. DMAP is not included in the plots as its concentration is much lower than the other species and it remains constant throughout.

estimates from prerun data can be used to facilitate rapid convergence of the iterative nonlinear fitting process.

There are several difficulties with the multivariate kinetic modeling approach to process monitoring and control; however, the benefits (discussed later) outweigh the difficulties in many circumstances. First, as in any model-fitting procedure, increasing the model complexity will improve the quality of the fit. In multivariate kinetic fitting, model complexity is increased by increasing the complexity of the reaction mechanism. This usually results in lower residuals for individual batches or experiments. Some method of model validation is necessary to guard against overfitting. In this paper, we used fitting of a kinetic model to several batches at significantly different conditions (different amount of catalyst, different reaction exotherms, and temperature profiles) to validate our model and guard against overfitting. While it is possible to find several reaction mechanisms (models) that give acceptable fits to individual batches, the likelihood is very low that the wrong mechanism will correctly fit other batches at significantly different conditions.

Another drawback of the multivariate kinetic modeling approach to process monitoring and control is that a significant amount of effort is required to elucidate the correct mechanism.

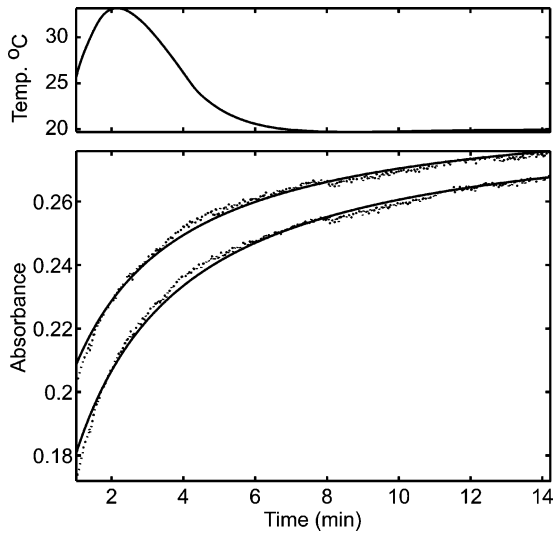

Figure 4. Temperature profile of the reaction and isothermal fits at 2202.9 (upper) and 2212.6 nm (lower) for 80.6 mg of DMAP. The dotted lines are the measured data and the solid lines the calculated data.

Table 3. Fitted Model Parameters for Batches 1−4[a]

A ($L^2mol^{-2}min^{-1}$)	E_A (kJ)
3.34×10^7 (1)	39.9 (2)

[a] Uncertainties are given in parentheses and represent two standard deviations of the last significant digit.

Table 4. Predicted and Fitted Concentrations for Batch 5 after 15.67 min

	predicted (mol/L)	fitted (mol/L)	error (%)
acetic anhydride	2.81	2.76	1.81
butanol	2.73	2.68	1.87
acetic acid and butyl acetate	2.60	2.65	1.89

Table 5. Comparison of Results Following Addition of the Adulterated Batch

	A ($L^2\ mol^{-2}\ min^{-1}$)	E_A (kJ)	SD of residuals
5 batches	1.94×10^7 (1)	38.5 (2)	1.13×10^{-3}
5 batches + adulterated batch	1.96×10^{12} (2)	68.5 (4)	2.30×10^{-3}

Multiple batches or experiments are required. Good experimental designs must be used with sufficiently different levels of controlled variables to unambiguously identify the correct mechanism and provide sufficient information to unambiguously identify and estimate all important model parameters. Inadequate designs will result in confounded model parameters. Sometimes many different reaction mechanisms must be tried until the best mechanism is found.

The benefits of multivariate kinetic modeling approach to process monitoring and control however are significant. Fitting multivariate kinetic models gives fundamental process insights. We have shown that including important information in the model such as the amount of catalyst and temperature gives robust

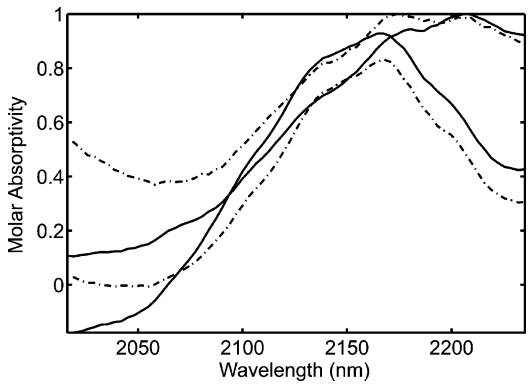

Figure 5. Spectra for the 80.6-mg batch. The solid lines show the estimated pure component spectra for the five good batches. The dash−dot lines show estimated pure component spectra of the adulterated batch. Spectra were normalized to 1 to facilitate visual comparison.

models that accurately estimate reaction profiles and reaction yields over a wide range of operating conditions. The time-dependent concentration profiles of species not directly observable in the spectroscopic measurements can be inferred from the model. For example, a catalyst may be present at concentrations too low to be analytically detectable, or there may be a lack of useful absorption bands in the range studied. In this paper, we have shown that the effect of a catalyst, however, can still be elucidated if a sufficient number of properly designed experiments are included in a multiway kinetic model.

The multivariate kinetic modeling approach is sensitive to the initial concentrations of reagents and reagent purity. Accurate values of the initial concentrations of reagents must be obtained from the amounts of reagents used to charge the reactor. This sensitivity, however, allows for very rapid and sensitive detection of process upsets caused by impurities. When process upsets occur, inspection of model results (estimated rate constants, spectral residuals, and estimated pure component spectra) can be compared to results from prior batches to give useful diagnostic information. For example, changes in estimated rate constants may indicate a significant change in catalyst activity, catalyst purity, or the presence of a different reaction mechanism from contamination, such as water as shown in this paper. A significant increase in spectral residuals can also indicate the presence of contamination. The appearance of new unexpected absorption bands in estimated pure component spectra can give diagnostic information and help identify the source of contamination.

Last, in multiway kinetic fitting, the use of one global kinetic model and different local spectral models for individual batches offers significant advantages (discussed below). One drawback of this approach is that the estimated concentration matrices of the batches, $\mathbf{C}_i$, are usually rank deficient. For example, in the reaction A + B → C + D, both reactants A and B disappear at the same rate and both products are formed at the same rate. Although the matrix **C** has four columns, its rank is only 2. This means the solution to eqs 5 and 6 must be solved at lower rank, and only two "pure component" spectra are estimated. The estimated spectra thus represent "pseudospecies", where the spectra of the two pseudospecies represent the sum of the pure component spectra, A + B and C + D, respectively.

The advantage gained by using different local spectral models for individual batches is significant, however. We have shown in this paper that different baseline offsets or even small shifts in spectral response from batch to batch do not seriously impact the quality of the calibration-free kinetic models. These batch-to-batch differences appear as small differences in the estimated pure component spectra. As long as the time variant spectral response gives adequate information to accurately and precisely estimate the model parameters, excellent calibration-free estimates of time-dependent concentration profiles are obtained. This represents a significant advantage compared to traditional multivariate calibration approaches such as PLS, where small changes in a spectrometer's response caused by changing a burned-out lamp or replacing a damaged fiber-optic probe or cable can invalidate a calibration model.

ACKNOWLEDGMENT

P.G. acknowledges that this research was supported in part by a grant from the National Science Foundation (CHE-0201014) and a grant from the Measurement and Control Engineering Center (MCEC) at the University of Tennessee, Knoxville, TN.

Received for review November 15, 2003. Accepted February 23, 2004.

AC035356I